

## Large eddy simulation of flow past a circular cylinder at Reynolds number 3900

W. Sidebottom<sup>1</sup>, A. Ooi<sup>1</sup> and D. Jones<sup>2</sup>

<sup>1</sup>Department of Mechanical Engineering  
The University of Melbourne, Victoria, 3010 AUSTRALIA

<sup>2</sup>Hydrodynamics Group, Maritime Platforms Division  
Defence Science and Technology Organisation, Fishermans Bend, 3207 AUSTRALIA

### Abstract

The flow past circular cylinders at a subcritical Reynolds number of 3900 has been studied extensively, both experimentally and numerically. This makes it an ideal test case for validation of numerical techniques. Results from large eddy simulations with two different subgrid scale models are presented and compared to the experimental results of Ong and Wallace [11], Lourenco and Shih [7] and Norberg [10]; and the numerical data of Kravchenko and Moin [6] and Beaudan and Moin [1]. The results are obtained by solving the incompressible Navier–Stokes equations using a finite volume method. The subgrid scale models—one equation eddy viscosity and Smagorinsky—show good agreement with the aforementioned experimental and computational results. The one equation eddy viscosity model, however, provides more accurate results in general.

### Introduction

This paper presents simulations of the flow over a circular cylinder at a subcritical Reynolds number based on the diameter of 3900. Flow over cylinders has been studied extensively, both numerically and experimentally, and is the subject of several comprehensive reviews, such as those provided by Beaudan and Moin [1], Kravchenko and Moin [6], and Ma *et al.* [8]. Studies of the flow phenomena in the cylinder wake are conducted for many reasons, from direct application in industrial engineering to validation of numerical schemes. The purpose of this study is to validate the LES procedure employed by *OpenFOAM* and to assess the accuracy of the two subgrid scale (SGS) models.

Several computational techniques have been used to study this flow, including: those based on the Reynolds–Averaged Navier–Stokes (RANS) and unsteady Reynolds–Averaged Navier–Stokes (URANS) equations [14]; large eddy simulations (LES) [1, 2, 6, 8]; and direct numerical simulations (DNS) [8]. RANS models are based on an averaging process whereby the independent variables of the Navier–Stokes equations, such as  $u$  and  $p$ , are decomposed into an average part and a fluctuating part—known as the Reynolds decomposition. The averaged equations therefore neglect the turbulent structures in the flow, which have to be modelled by additional equations. URANS methods are similar to RANS methods, with the addition of a time-dependent term in the governing equations. LES applies a filter to the governing equations, which acts to resolve only the large-scale structures in the flow. Therefore, additional equations are again required to model the small-scale features of the flow. DNS resolves all scales in the flow, which results in high accuracy and high computational cost. LES, therefore, is a compromise between RANS, or URANS, and DNS, and is chosen here to obtain reasonable accuracy with modest computational resources. Additionally, RANS methods are generally unable to predict the complex separated flow over circular cylinders [14].

There is no universal way to characterise the flow regimes in the wake of a circular cylinder, however, the review by Beaudan and

Moin [1] provides a comprehensive discussion of one possible method. At Reynolds numbers less than about 40, the flow is steady, laminar and symmetrical [12]; between 40 and 150 the flow remains laminar and is associated with a regular vortex shedding frequency, which increases with Reynolds number; at approximately 180 the flow becomes three-dimensional in the near wake; and between 300 and  $2 \times 10^5$  the flow around the surface of the cylinder is laminar and there is transition to turbulence in the separated free shear layers. The range between 300 and  $2 \times 10^5$  is known as the subcritical range, and is the subject of the present study. For lower Reynolds numbers in this range, the wake is fully turbulent 30 to 40 diameters downstream of the cylinder, and for the higher Reynolds numbers, the wake is fully turbulent close to the rear of the cylinder. Reynolds numbers between  $2 \times 10^5$  and  $3.5 \times 10^6$  are classified as the critical range [1].

Just as there is no universal way to characterise the flow regimes, there is no established means by which to define the different regions in the cylinder wake. Henceforth, the convention adopted by Ma *et al.* [8] will be employed. In this, the near wake, defined as less than ten diameters aft of the cylinder (*i.e.*  $x/D < 10$ ), is subdivided into the *very near wake* ( $x/D < 3$ ) where the dynamics of the shear layer dominate, and the *near wake* ( $3 < x/D < 10$ ).

The choice of Reynolds number for this study was motivated by several factors. First, flow in the subcritical range features several interesting phenomena, including: a laminar boundary layer with unsteady separations and reattachments; flow reversals at the cylinder surface and in the near wake; adverse pressure gradients; transitioning free shear layers; and a turbulent wake with random and periodic Reynolds stresses [1]. Second, there is data from two separate experiments, which provide measurements of the velocity and Reynolds stresses in the cylinder wake. Lourenco and Shih [7] performed Particle Image Velocimetry to obtain mean and phase-averaged data within three diameters downstream, and Ong and Wallace [11] made single sensor measurements of mean velocities and Reynolds stresses in the wake between the closure point of the recirculation bubble and ten diameters aft of the cylinder. Third, and finally, there is an abundance of data from numerical simulations—particularly LES—for comparison [1, 2, 6, 8, 14].

### Previous Computational Results

An overview of widely cited LES studies of the cylinder wake at Reynolds number 3900 is presented in [5]. A short précis of this will be provided here. The aforementioned simulations of Beaudan and Moin [1] solved the compressible Navier–Stokes equations on an O-grid with a high-order upwind scheme, which was found to be very dissipative in regions where the mesh coarsened. Mittal and Moin [9], then, performed LES of incompressible flow on a C-mesh with a second-order central difference scheme. The mean flow results of this study were similar to those of Beaudan and Moin, however, the power spec-

Data from	$\bar{C}_D$	$-C_{P_b}$	$St$	$\theta_{sep}$	$L_{rec}/D$	$\bar{U}_{min}$
Experiment	$0.99 \pm 0.05$	$0.88 \pm 0.05$	$0.215 \pm 0.005$	$86.0^\circ \pm 2$	$1.4 \pm 0.1$	$-0.24 \pm 0.1$
Kravchenko and Moin [6]	1.04	0.974	0.210	$88.0^\circ$	1.35	-0.37
One equation eddy	0.89	0.93	0.179	$85.5^\circ$	1.19	-0.29
Smagorinsky	0.86	0.93	0.179	$80.1^\circ$	1.09	-0.28

Table 1: Flow parameters from the present simulations compared to other computational and experimental results (as in [6]). The experimental value of  $-C_{P_b}$  is from [10] at  $Re_D = 4020$ ;  $St$  is from [11] at  $Re_D = 3900$ ;  $L_{rec}/D$  is from [4] at  $Re_D = 3900$ ;  $\theta_{sep}$  is from [13] at  $Re_D = 5000$ ; and  $\bar{U}_{min}$  is from [7] at  $Re_D = 3900$ .

tra in the near wake were in better agreement with the experimental results [11]. Kravchenko and Moin [6] performed LES of incompressible flow on an O-grid with a high-order scheme based on B-splines and achieved even better agreement with the experimental power spectra. This study also predicted a larger recirculation zone than that obtained from the experiment of Lourenco and Shih [7]. Breuer [3] used a finite volume method with central differences to solve the incompressible equations on an O-grid and found a shorter recirculation length than did Lourenco and Shih. All studies have found that the flow around a cylinder at a Reynolds number of 3900 is very sensitive to the boundary conditions, small disturbances caused by insufficient resolution, and freestream turbulence.

### Governing Equations and Numerical Method

The governing equations used for this study are the incompressible Navier–Stokes equations. As mentioned previously, large eddy simulations use a filter to partition the turbulent flow into a resolved scale and a subfilter, or subgrid scale (SGS). A resolved-scale variable  $\bar{\phi}$  is defined as:

$$\bar{\phi}(x) = \int_D G(x,y)\phi(y)dy \quad (1)$$

where  $D$  is the entire flow domain and  $G$  is a spatial filter, which removes high spatial-frequency information [1]. The equations obtained after filtering the incompressible Navier–Stokes equations are shown in Blackburn and Schmidt [2].

The momentum flux,  $\overline{u_j u_i}$ , on the left-hand side of the filtered equations is nonlinear and cannot be found in terms of the resolved components  $\bar{u}_i$ . Therefore, similar to the way the nonlinear term is modelled in RANS equations, this term is decomposed into resolvable and modelled components such that  $\overline{u_j u_i} = \bar{u}_j \bar{u}_i + [\overline{u_j u_i} - \bar{u}_j \bar{u}_i]$  and  $[\overline{u_j u_i} - \bar{u}_j \bar{u}_i]$  is known as the *subgrid scale stress tensor*,  $\tau$ . The momentum equation is then:

$$\frac{\partial \bar{u}_i}{\partial t} + \frac{\partial}{\partial x_j} (\bar{u}_j \bar{u}_i) = -\frac{1}{\rho} \frac{\partial \bar{p}}{\partial x_i} + \nu \frac{\partial^2 \bar{u}_i}{\partial x_j \partial x_j} - \frac{\tau_{ij}}{\partial x_j} \quad (2)$$

and it is the task of the SGS model to predict  $\tau$  based on the resolved scale velocity,  $\bar{u}_i$ . Two SGS models are used in this study—the one equation eddy viscosity model and the Smagorinsky model.

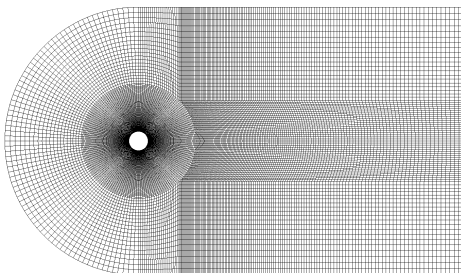


Figure 1: The computational mesh used for the simulations.

The one equation eddy viscosity SGS model uses a differential equation to simulate the behaviour of the SGS kinetic energy,  $k$ . This is shown in equation (3).

$$\frac{dk}{dt} + \nabla \cdot (\mathbf{u}k) - \nabla \cdot [(\mathbf{v} + \mathbf{v}_{sgs})\nabla k] = 2\mathbf{v}_{sgs} \left[ \frac{1}{2}(\nabla \mathbf{u} + \nabla \mathbf{u}^T) \right]^2 - \frac{1}{\Delta} c_e k^3/2 \quad (3)$$

Here,  $\Delta$  is the filter width,  $\nu$  is the kinematic viscosity of the freestream, and

$$\mathbf{v}_{sgs} = c_k k^{1/2} \Delta \quad (4)$$

is the SGS viscosity. The constants  $c_e$  and  $c_k$  were given the *OpenFOAM* default values of 1.048 and 0.094, respectively.  $\mathbf{v}_{sgs}$  is similar to the turbulent or eddy viscosity commonly used in turbulence models derived from the Boussinesq approximation in RANS analysis. Here, it is similarly used to calculate the subgrid scale stress tensor,  $\tau$ , as shown in equation (5):

$$\tau = -\mathbf{v}_{sgs} [\nabla \mathbf{u} + \nabla \mathbf{u}^T] + \frac{2}{3} \mathbf{I}k \quad (5)$$

where  $\mathbf{I}$  is the identity matrix.

The implementation of the Smagorinsky SGS model in *OpenFOAM* is somewhat dissimilar to the typical implementation, such as that used by Blackburn and Schmidt [2]. Here, the SGS kinetic energy is found using equation (6).

$$k = 2 \frac{c_k}{c_e} \Delta^2 \left\{ \frac{1}{2}(\nabla \mathbf{u} + \nabla \mathbf{u}^T) - \frac{1}{3} tr \left[ \frac{1}{2}(\nabla \mathbf{u} + \nabla \mathbf{u}^T) \right] \right\}^2 \quad (6)$$

And the SGS viscosity is calculated as:

$$\mathbf{v}_{sgs} = c_k \Delta [k \nabla \mathbf{u}]^{1/2} \quad (7)$$

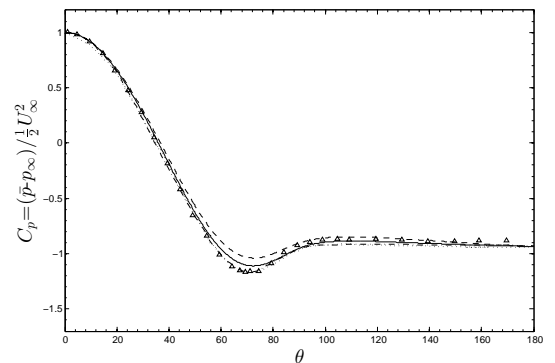


Figure 2: Pressure coefficient on the cylinder surface: —, one equation eddy; ---, Smagorinsky;  $\triangle$ , experiment of Norberg [10]; - · -, B-spline simulations [6].

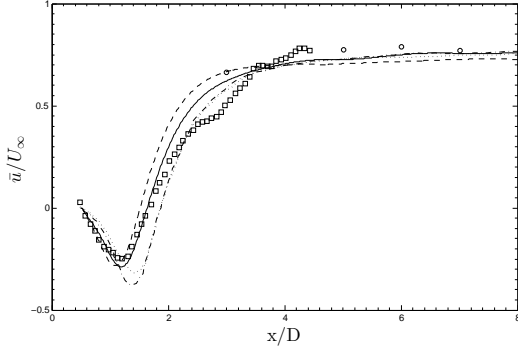


Figure 3: Time mean streamwise velocity on the wake centreline: —, one equation eddy; ---, Smagorinsky;  $\square$ , experiment of Lourenco and Shih [7];  $\circ$ , experiment of Ong and Wallace [11]; - · - ·, B-spline simulations [6]; · · ·, upwind simulations [1].

The constants  $c_k$  and  $c_e$ , and the filter width,  $\Delta$  have the same values and meaning as they did in the one equation eddy viscosity model. The result for the SGS viscosity is then used in equation (5) to calculate the SGS stress tensor.

The discretisation scheme used in LES plays a dominant role in the quality of the solution. The effect of the discretisation scheme was studied by Breuer [3], who performed simulations with five different numerical schemes and with dynamic and Smagorinsky SGS models. Breuer concluded that simulations conducted with central differencing schemes were in better agreement with experimental results than those conducted with dissipative methods, such as upwind differencing. This conclusion was in agreement with the findings of previous studies [1, 9]. Indeed, in all studies, it was found that low-order upwind schemes could not predict the size of the recirculation zone, the base pressure coefficient, or the separation angles accurately. Additionally, Breuer concluded that the numerical dissipation produced by a scheme is more crucial for LES than its formal order of accuracy [3]. As a result of these findings, central differencing was used to discretise the divergence terms in the governing equations for the present simulations.

The mesh used for the simulations is shown in figure 1 and contains 1,929,600 hexahedral control volumes. This is more than Franke and Frank [5] (1,138,688), Kravchenko and Moin [6] (1,333,472), and Blackburn and Schmidt [2] (855,040), but less than Young and Ooi [14] (4,320,000). The spanwise ex-

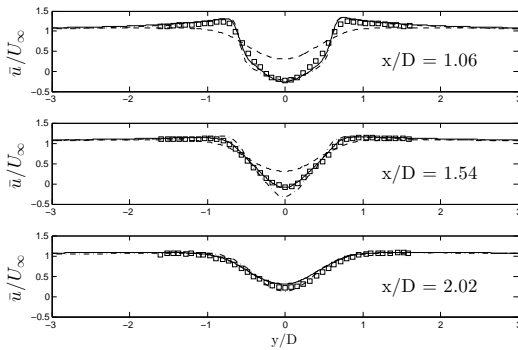


Figure 4: Mean streamwise velocity at three locations in the very near wake: —, one equation eddy; ---, Smagorinsky;  $\square$ , experiment of Lourenco and Shih [7]; - · - ·, B-spline simulations [6].

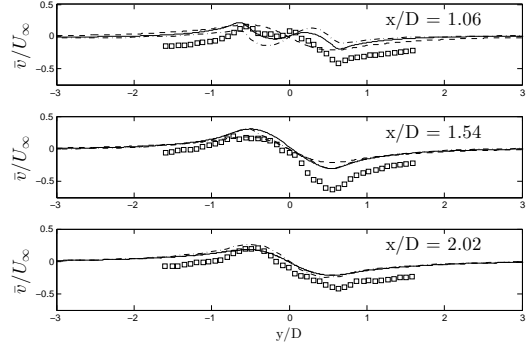


Figure 5: Mean cross-flow velocity at three locations in the very near wake: —, one equation eddy; ---, Smagorinsky;  $\square$ , experiment of Lourenco and Shih [7]; - · - ·, B-spline simulations [6].

tent of the domain was chosen to be  $L_z/D = \pi$  in accordance with many previous studies [1, 2, 6, 8, 14]. Ma *et al.* varied the spanwise extent as  $L_z/D = \pi/2, \pi, 3\pi/2$  and  $2\pi$  and found no significant improvement in results beyond  $L_z/D = \pi$ , provided the resolution remained the same [8]. The domain extends  $\pm 7D$  in the vertical (or cross-flow) direction,  $-7D$  in the inflow, and  $17D$  in the outflow. In accordance with Beaudan and Moin [1], Mittal and Moin [9] and Kravchenko and Moin [6], 48 grid points are used in the spanwise direction. This is significantly more than the number of grid points used by Franke and Frank [5] and Breuer [3], who used 33; and Blackburn and Schmidt [2], who used 32 in the same direction. The study of LES results by Young and Ooi [14] shows that no significant improvement is made by increasing the spanwise resolution from 32 to 48 grid points. The choice of 48 grid points, therefore, was made for consistency only.

The inflow condition was specified to be equal to the freestream velocity,  $U_\infty$ , with a turbulence intensity of 2% and a Neumann condition for the pressure (*i.e.* zero gradient). The outflow condition was specified to change the velocity between the freestream value and zero gradient depending on its direction to allow for flow recirculation at the boundary. The pressure at the outflow was specified as the freestream value. The front and back faces of the mesh were given a periodic boundary condition. The simulations were allowed to reach a statistically steady state before any data was collected. The data were then averaged in time and across twenty planes in the span-

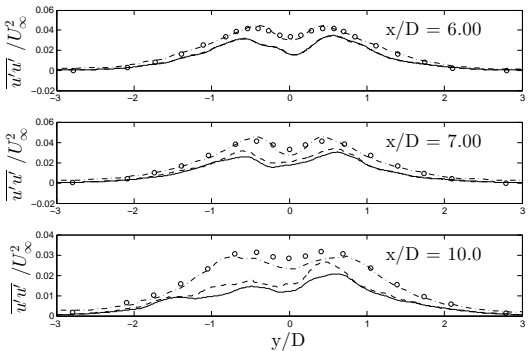


Figure 6: Velocity fluctuation covariance at three locations in the near wake: —, one equation eddy; ---, Smagorinsky;  $\circ$ , experiment of Ong and Wallace [11]; - · - ·, B-spline simulations [6].

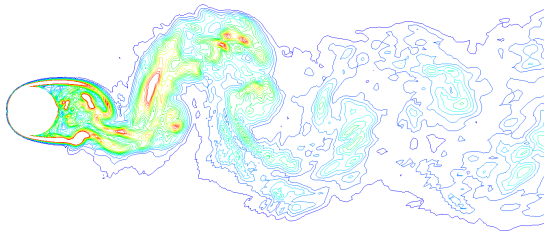


Figure 7: Instantaneous vorticity magnitude contour plot of the Smagorinsky method. Shown are 16 contours from  $\omega D/U_\infty = 0.5$  to  $\omega D/U_\infty = 10.0$ .

wise direction. In accordance with previous studies, statistics were collected over approximately seven vortex shedding cycles ( $T = 35D/U_\infty$ ) [1, 6]. The simulations were run with a variable timestep and a fixed Courant number of 0.75 to ensure stability.

### Results

Some of the key flow parameters for flow over a circular cylinder are shown in table 1. Comparisons are made between the results from this study, experimental results, and the results from the B-spline simulations of Kravchenko and Moin [6]. Although not all of the results agree within experimental uncertainty, the results from the one equation eddy SGS model are generally in better agreement than those from the Smagorinsky model. This is also true for the results shown in figures 2–6.

Figure 2 shows the pressure distribution over the surface of the cylinder. Both SGS models show close agreement with the comparison data, however, the one equation eddy model is more accurate, especially near the separation region—as shown by the value of  $\theta_{sep}$  in table 1. Figure 3 shows the time mean streamwise velocity along the wake centreline. Both SGS models predict a shorter recirculation region,  $L_{rec}/D$ , than that predicted by the simulations of [1] and [6]. This prediction is, however, in close agreement with the experiment of Lourenco and Shih [7]. All simulations and experiments tend to the same value of  $\bar{u}/U_\infty$  as  $x/D$  becomes large. Figures 4 and 5 show the predicted mean streamwise and cross-flow velocity, respectively, at three locations in the near wake. The results of the one equation eddy SGS model again show good agreement with the comparison data. The Smagorinsky model fails to predict the minimum streamwise velocity in figure 4 at each wake location; and also fails to predict the double hump in the cross-flow velocity near the wake centreline in figure 5. At the furthest wake location,  $x/D = 2.02$ , both models agree well with the comparison data. Figure 6 shows the covariance of the velocity fluctuations in the near wake. At  $x/D = 6.00$ , both simulations show a reasonable agreement with the comparison data. However, at wake locations further from the cylinder, the profiles become more dissimilar to the comparison data. This is likely due to the coarsening of the computational grid further from the cylinder, as is evident in figure 1.

Figure 7 shows instantaneous vorticity magnitude contours from the Smagorinsky SGS model. As expected, two long separating shear layers are present and the development of the Kármán vortex street is evident. The Kármán vortex street becomes less clear further from the cylinder. This is again likely due to the coarsening of the computational grid as  $x/D$  increases.

### Conclusions

This paper has provided a short, yet thorough overview of the extensive literature associated with flow around a circular cylinder

at Reynolds number 3900. Based on this appraisal, simulations were set up to be consistent with predominate previous LES studies. The results from both subgrid scale models were shown to be in good agreement with the data from other simulations and experiments, with the exception of the velocity fluctuation covariance as  $x/D$  becomes large. The one equation eddy model was shown, however, to more accurately predict the complex flow phenomena emanating from the cylinder than the Smagorinsky model.

### References

- [1] Beaudan, P. and Moin, P., Numerical experiments on the flow past a circular cylinder at sub-critical Reynolds number. In *Tech. Rep. TF-62*, Dept. Mech. Engng, Stanford University, 1994.
- [2] Blackburn, H. and Schmidt, S., Large eddy simulation of flow past a circular cylinder. *Proceedings of the Fourteenth Australasian Fluid Mechanics Conference*, Adelaide University, 2001, 689-692.
- [3] Breuer, M., Numerical and modelling influences on large eddy simulations for the flow past a circular cylinder, *Int. J. Heat Fluid Fl.*, **19**, 1998, 512-521
- [4] Cardell, G., *Flow past a circular cylinder with a permeable splitter plate*. PhD thesis, Graduate Aeronautical Laboratories, California Institute of Technology, 1993.
- [5] Franke, J. and Frank, W., Large eddy simulation of the flow past a circular cylinder at  $Re_D = 3900$ , *J. Wind Eng. Ind. Aerod.*, **90**, 2002, 1191-1206.
- [6] Kravchenko, A. G. and Moin, P., Numerical studies of flow over a circular cylinder at  $Re_D = 3900$ , *Phys. Fluids*, **12**, 2000, 403-417.
- [7] Lourenco, L. M. and Shih, C., Characteristics of the plane turbulent near wake of a circular cylinder. A particle image velocimetry study. Reported in [6].
- [8] Ma, X., Karamanos, G., and Karniadakis, G., Dynamics and low-dimensionality of a turbulent near wake, *J. Fluid Mech.*, **410**, 2000, 29-65.
- [9] Mittal, R. and Moin, P. Large-eddy simulation of flow past a circular cylinder, *APS Bulletin*, **41**(9), 49th DFD Meeting, 1996.
- [10] Norberg, C. Effects of Reynolds number and low-intensity free stream turbulence on the flow around a circular cylinder. In *Publ. No. 87/2*, Chalmers University of Technology, Gothenburg, Sweden, 1987.
- [11] Ong, L. and Wallace, J., The velocity field of the turbulent very near wake of a circular cylinder, *Exp. Fluids*, **20**, 1996, 441-453.
- [12] Roshko, A., On the development of turbulent wakes from vortex streets, *NACA Technical Note 1191*, 1954, 1-25.
- [13] Son, J. and Hanratty, T., Velocity gradients at the wall for flow around a cylinder at Reynolds numbers  $5 \times 10^3$  to  $10^5$ , *J. Fluid Mech.*, **35**, 1969, 353.
- [14] Young, M. and Ooi, A. Comparative assessment of LES and URANS for flow over a cylinder at a Reynolds number of 3900. *Proceedings of the Sixteenth Australasian Fluid Mechanics Conference*, The University of Queensland, 2007, 1063-1070.